Electronic Supplementary Material (ESI) for RSC Advances.

Supporting information

Evidence of Enhanced Photocurrent Response in Corannulene Films

Nadiia Pastukhova[1], L. Martin Samos[1,2], Laura Zoppi[3], Egon Pavlica[1], Jinta Mathew[1], Gvido Bratina,[1] Kim K. Baldridge[4], Jay S. Siegel[4]

[1] Laboratory of Organic Matter Physics, University of Nova Gorica, Vipavska 13, SI-5000 Nova Gorica, Slovenia

[2]CNR-IOM DEMOCRITOS, Istituto Officina dei Materiali, c/o SISSA Scuola Internazionale Superiore di Studi Avanzati, Via Bonomea 265, 34136 Trieste ITALY, [3] Department of Chemistry, University of Zürich, Winterthurerstrasse 190, CH-8057 Zürich

[4] Health Sciences Platform, Tianjin University, 92 Wejin Road, Nankai District Tianjin, 300072, P. R. China.

Table of Contents

Preparation of corannulene in a solution

Corannulene solutions were prepared in three different solvents: chloroform $CHCl_3$, dichloromethane CH_2Cl_2 (both Sigma-Aldrich) and a diethyl ether $(C_2H_5)_2$ (Alfa Aesar). These solvents were selected due to their relatively high transmissivity of UV light and good corannulene solubility. In order to ensure solubility and avoid molecule aggregation, each solution was additionally sonicated for 5 minutes in an ultrasonic bath before testing or before diluting to prepare lower concentrations. The corannulene concentration varied between 0.45 g/l and 26 g/l for each solvent.

UV/visible absorption of corannulene in solution

The UV/visible absorption spectra of corannulene solutions was obtained by a spectrophotometer (Perkin Elmer Lambda 650S) using a quartz cuvette (Hellma 114-QS) with a 10 mm light path. Clear solvents were measured for the background removal.

Each spectrum is reported as an average of 3 repetitions. Number of repetitions was chosen depending on the absorption level of a solution in order to reduce the noise to signal ratio. The absorption spectrum of corannulene in chloroform (CF), corannulene in dichloromethane (DCM) and corannulene in diethyl ether (DEE) are shown in Figs. S1-S3. Each spectrum exhibits a group of peaks in the energy range from 3.5 eV to 4.75 eV. The highest intensity peak for all spectra is centred around 4.3 eV with a shoulder on the high energy side. Shoulder occurs at the 4.5 eV and a low energy tail extends from 4.0 eV to 3.5 eV. To accurately determine the effect of solvent on the absorption features, each measured spectrum was modelled as a sum of four Gaussian peaks with the parameters provided in Table S1.

The evolution of absorption features was studied as a function of concentration of corannulene. The peak energies do not change with concentration. The oscillator strength, as expected, increases with concentration. Its dependence on the corannulene concentration (*c*) is presented in Fig. S4 in a double logarithmic plot. Symbols represent relative oscillator strength (*f*), obtained by spectra modelling with Gaussians, dashed line represents a power law model $f \propto c^{a}$. The power exponent is close to unity (0.96 ± 0.01), which demonstrates that the f is increasing with concentration only due to number of molecules in the solution. Based on f linear dependence we conclude that the corannulene molecules are not interacting and are fully dissolved.

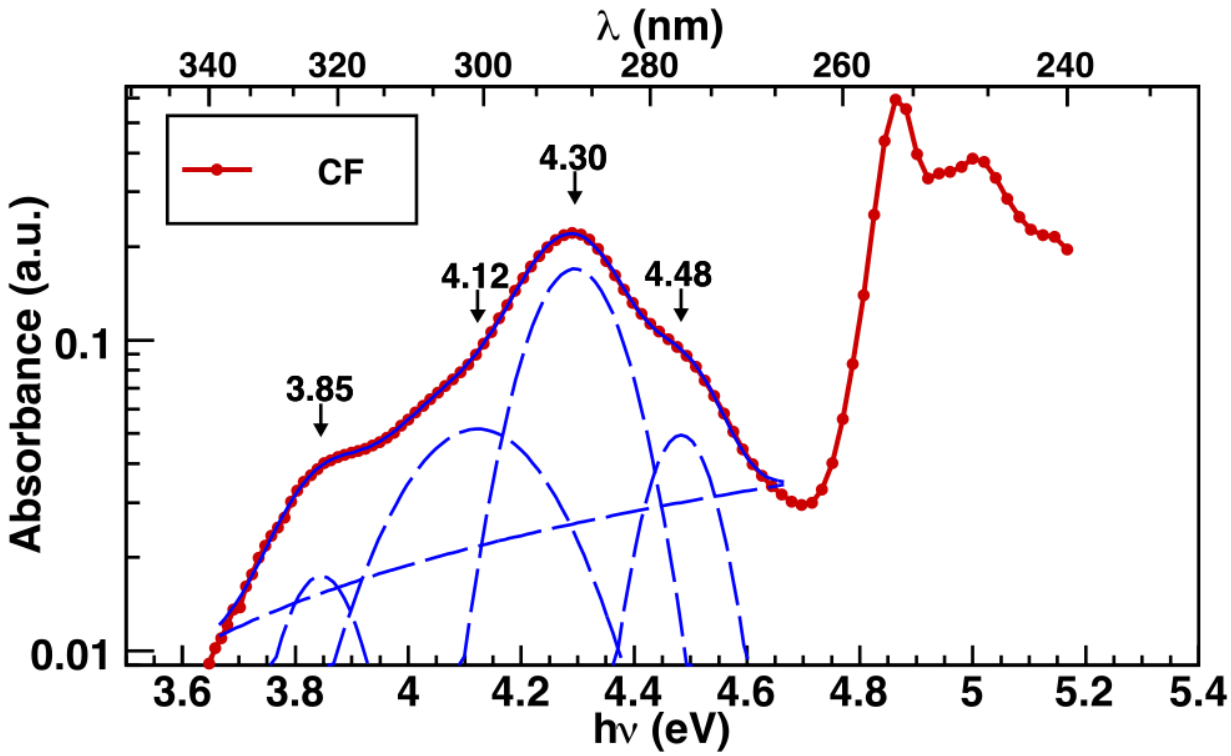

Figure S1: Optical absorption of corannulene dissolved in chloroform (CF). Concentration 10μg/ml.

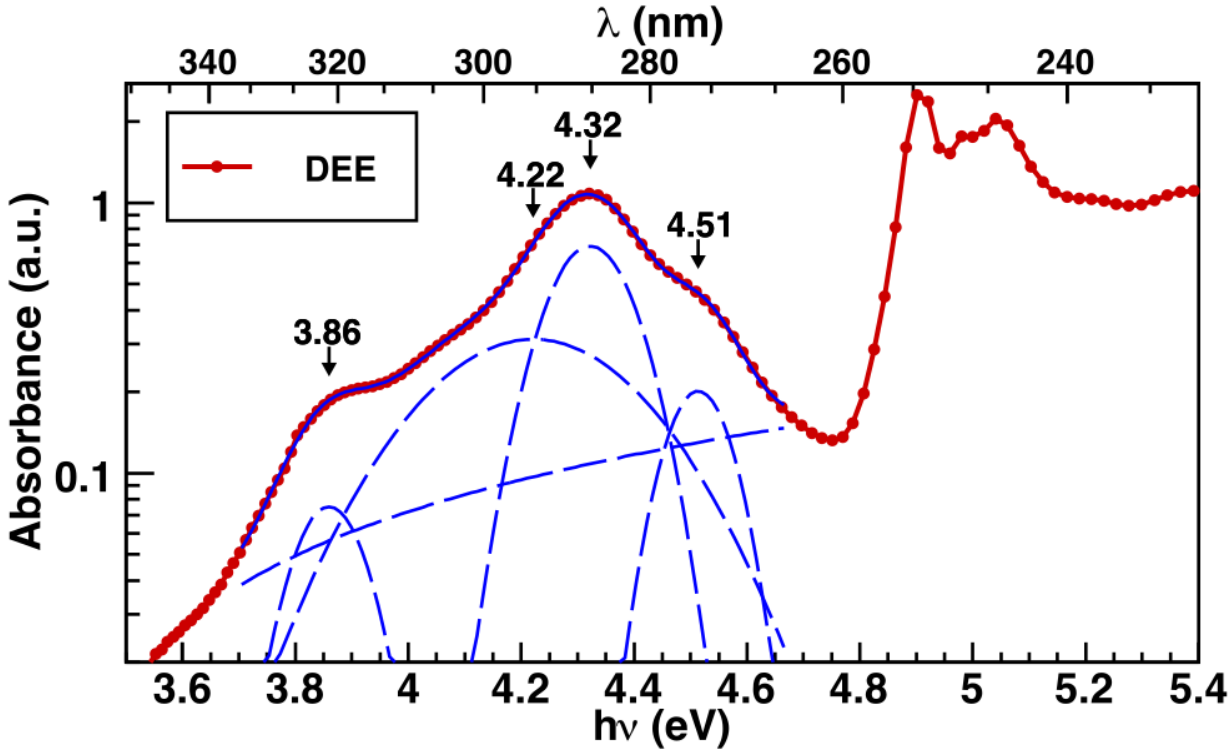

Figure S2: Optical absorption of corannulene dissolved in diethyl ether (DEE). Concentration 2.8 μg/ml.

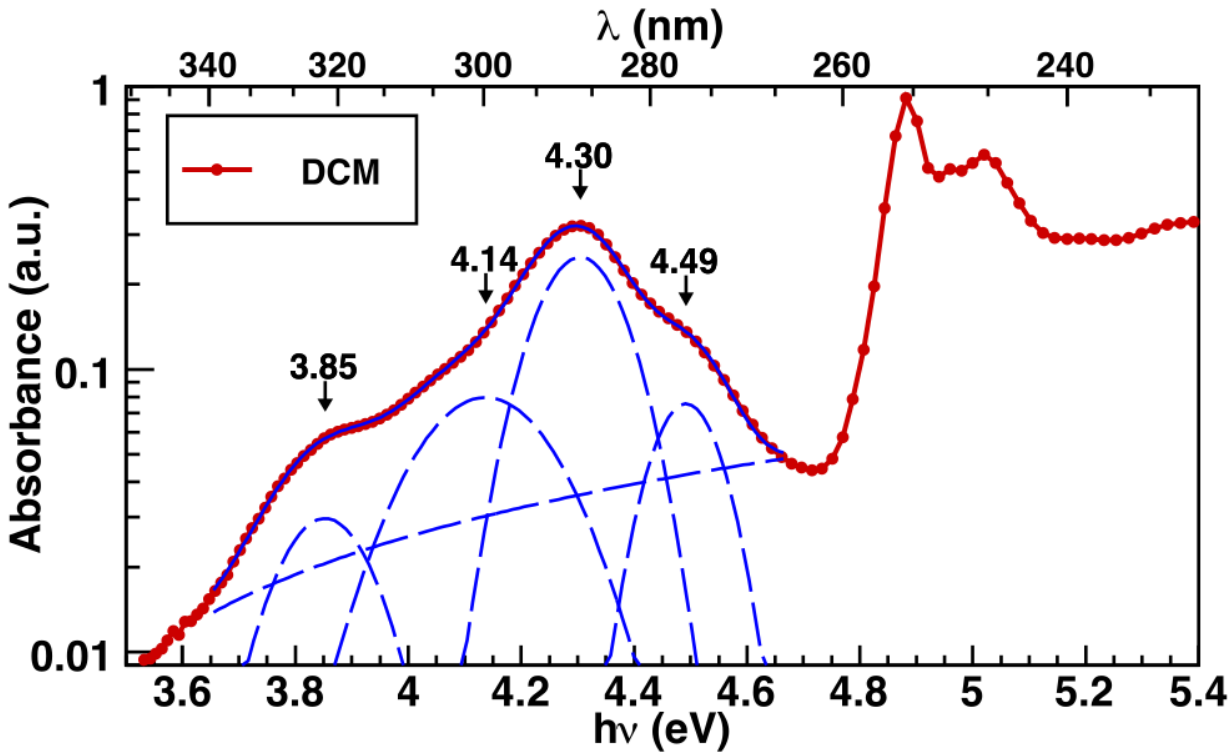

Figure S3: Optical absorption of corannulene dissolved in dichloromethane (DCM). Concentration 26 µg/ml.

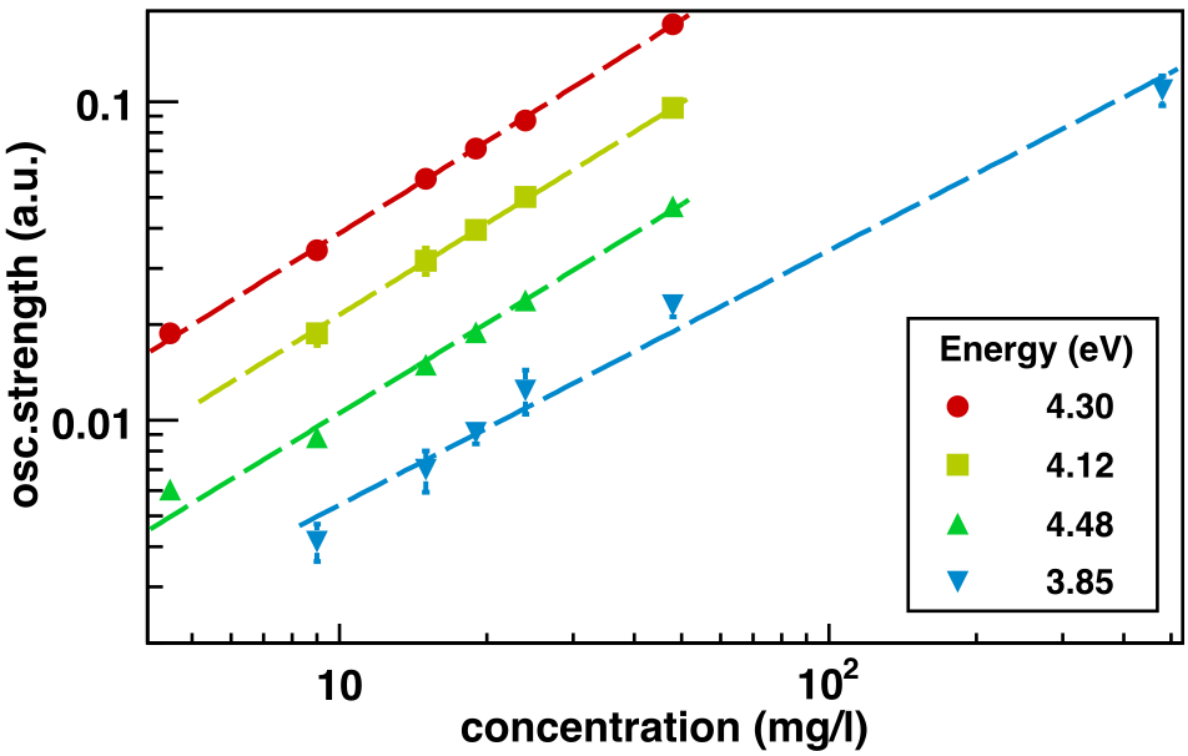

Figure S4: Relative oscillator strength (*f*) of optical absorption of corannulene as a function of concentration in chloroform solution (CF). Absorption energies correspond to values in Table S1. Dashed lines represent a power law dependence.

Table S1: Parameters of Gaussian peaks, which were used to model the measured optical absorption spectra of corannulene solutions. Gaussian parameters are reported in terms of energy, full-width-at-half-maximum (FWHM) and oscillator strength. Oscillator strength is calculated as the area under the Gaussian curve, FWHM corresponds to ≈2.355σ of Gaussian width parameter and the energy represents the Gaussian's center.

Chloroform (CF)

Energy (eV)	3.8453 ± 0.004	4.123 ± 0.011	4.29531 ± 0.0007	4.4834 ± 0.0018
Oscillator	0.003155 ± 0.00034	0.01781 ± 0.0017	0.03475 ± 0.0014	0.007795 ± 0.0003

strength (a.u.)				
FWHM (eV)	0.17031 ± 0.0078	0.3234 ± 0.023	0.19253 ± 0.0024	0.14807 ± 0.003

Diethyl ether (DEE)

Energy (eV)	3.8598 ± 0.0032	4.221 ± 0.021	4.3222 ± 0.0012	4.5135 ± 0.0017
Oscillator strength (a.u.)	0.01259 ± 0.0017	0.1518 ± 0.022	0.13473 ± 0.008	0.03068 ± 0.004
FWHM (eV)	0.1574 ± 0.011	0.4563 ± 0.035	0.18314 ± 0.003	0.14338 ± 0.0064

Dichloromethane (DCM)

Energy (eV)	3.8526 ± 0.004	4.1371 ± 0.003	4.30453 ± 0.0006	4.4919 ± 0.0016
Oscillator strength (a.u.)	0.006664 ± 0.0006	0.02551 ± 0.0004	0.05026 ± 0.0004	0.012465 ± 0.00054
FWHM (eV)	0.21071 ± 0.0097	0.30106 ± 0.007	0.18911 ± 0.0016	0.15486 ± 0.0039

Spin-coating of corannulene film and Atomic force microscopy

Corannulene films were prepared by spin-coating of 5.8 g/l corannulene solution in chloroform on quartz substrate. Solution was heated to 40ºC for 10 minutes and then immediately spin-coated. Spin-coating of 60 µl of solution on the 1 cm x 1 cm substrate was done at 1500 rpm for 60s using the acceleration of approximately 10000 rpm/s. In order to improve surface coverage, the spin-coating was repeated once overt the first layer with exactly the same parameters.

Spin-coating was performed in a nitrogen-filled glovebox at room temperature with H_20 and O_2 concentration below 10 ppm.

Topography image of spin-coated layers was obtained by Atomic Force Microscope (A.P.E. Research) operating in non-contact mode. Fig. S5 represents topography of an area of 12 µm x 12 µm of a corannulene layer. Corannulene molecules completely cover the substrate. The morphology exhibits elongated structures of approximately 0.1 µm large diameter. Their length and orientation appears relatively ordered on the scale below 5 µm. However, on larger scale, their orientation and length are randomly distributed. RMS of the area in Fig. S5 is 23 nm.

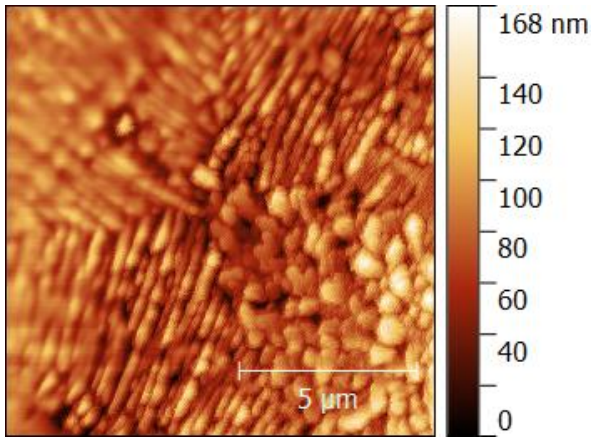

Figure S5: Atomic force microcopy of spin-coated corannulene layer.

Optical absorption of corannulene film

Corannulene thin films were prepared by spin-coating of the corannulene solution as described above. Absorption measurements were performed using the spectrophotometer Perkin Elmer Lambda 650S. As reference a clean quartz substrate was used and its absorption was subtracted from the absorption of corannulene covered quartz. In order to test reproducibility several samples were prepared and characterized. We submit that the absorption spectra of single and

double spin-coated samples exhibit similar peak positions, but varying magnitude, which presumably originates from the thickness variation. The absorption spectrum of a spin-coated thin film of corannulene is shown in Fig. S6. The spectrum has 2 group of peaks. The first group includes main peaks at 3.68 eV and 4.06 eV, while the second group comprises resolved peaks at 4.8 eV, 5.04 eV and 5.45 eV. We note that more peaks can be added to the model in order to fine-tune the shape of spectrum.

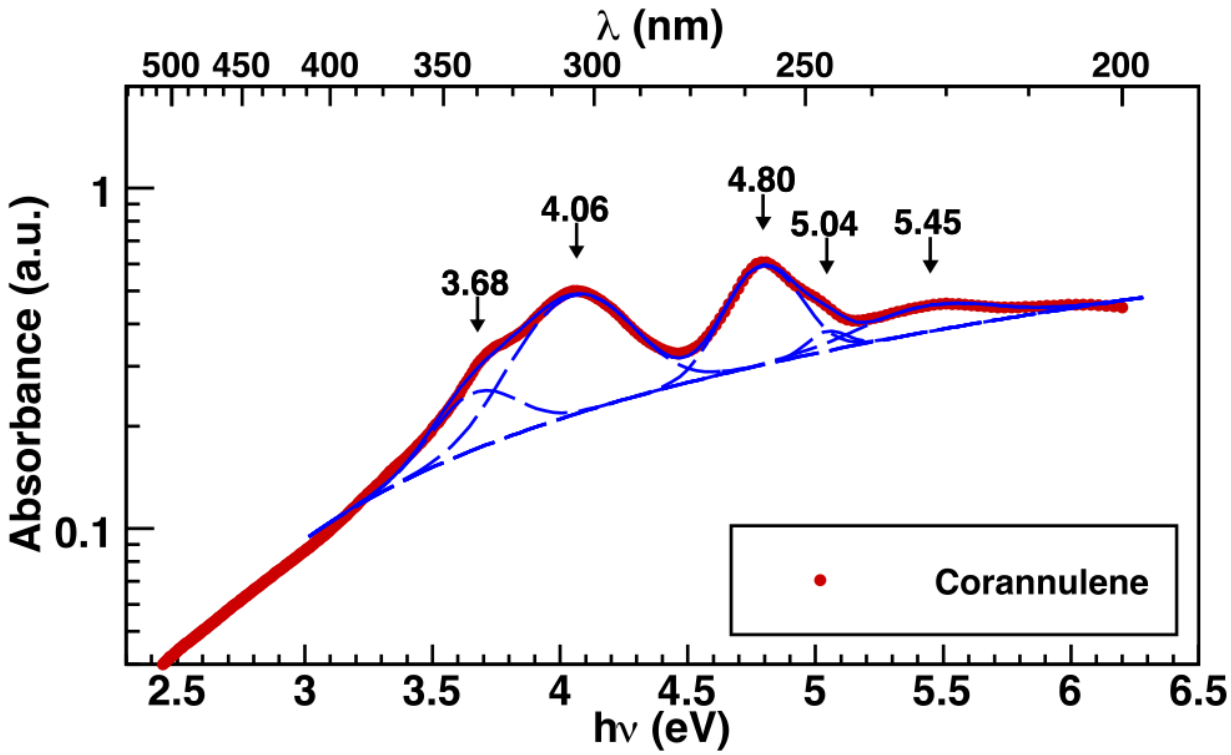

Figure S6: Optical absorption of the corannulene spin-coated film (solid line). The spectrum was modeled (dashed line) as a sum of Gaussians centered at 3.68 eV, 4.06 eV, 4.8 eV, 5.04 eV, 5.45 eV and a background signal. The absorption background signal is modeled as a straight dashed line.

Time-of-flight (TOF) photoconductivity measurement with a coplanar electrodes setup

TOF photoconductivity method (Fig. S7) was used to measure the photoconductivity of spin-coated corannulene layers. Experimental setup is described in Refs.[1-5]. In details, two coplanar 100 nm thick Au electrodes were vacuum-deposited through shadow mask onto the quartz substrate prior to corannulene spin-coating. The interelectrode distance was typically in the range between 50 – 200 μm. TOF measurements were performed by applying DC voltage (V_b) ranging from -500 V to 500 V between electrodes as schematically shown in Fig. S7. The biased electrode was connected also to the current amplifier through a bias-t element (Particulars BT-01), which is used to decouple transient photocurrent response from the constant dark current. Schematically it is depicted as pair of capacitor (C) and inductor (L) in Fig. S7. Charge carriers were generated using a pulsed laser of a tunable photon energy between 3.5eV (350 nm) and 5.9 eV (210 nm), pulse duration of 3 ns and repetition rate of 10 Hz. The laser light was focused near the biased electrode in the direction normal to the sample surface. Laser pulse intensity was attenuated to ensure that the total charge (the time integral of the photocurrent pulse) was less than 10% of the total capacitor charge and hence the photogenerated charge could not screen the external electric field. The photocurrent transients I(t) were amplified by a 2 GHz current amplifier (Particulars AM-01A) and recorded by a 2.5 GHz oscilloscope (Lecroy, WavePro 725i). Au electrodes were connected to bias-t and current amplifier by 4GHz probe tips (Signatone SP-100). Sample preparation and all measurements were performed in a nitrogen-filled glovebox at room temperature with H_20 and O_2 concentration below 10 ppm.

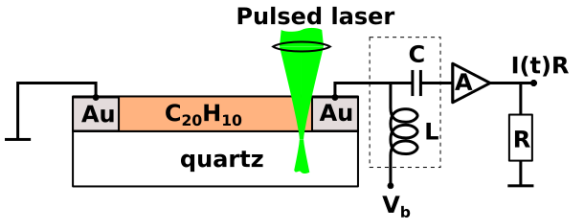

Figure S7: Schematic view of the time-of-flight photoconductivity measurement with coplanar electrode setup. Corannulene layer is deposited on top of quartz substrate.

Photon-corannulene interaction results in free photogenerated charge carriers, which drift toward metal electrodes due to externally applied electric field. The drift of carriers induces electric current - photocurrent I(t) - to the electrode due to displacement field according to the Shockley-Ramo theorem[6-9]. Time integration of I(t) corresponds to the amount of photogenerated carriers that reach the electrodes (N_e). N_e depends on the photon-to-charge carrier conversion efficiency and the probability that the carrier does not trap or recombine during its transport. The transport efficiency is proportional to the carrier mobility, which in turn depends on the overlap of the molecule orbitals. Hence, we present the corannulene photoconductivity as a ratio between the number of collected photogenerated charge carriers (N_e) and the number of incident photons for each light pulse (N_{ph}). The ratio is known as the external quantum efficiency (EQE). EQE was measured as a function of photo-excitation energy. For each photon energy, EQE is reported as an average of 1000 pulses. For each light pulse, N_e is obtained by time integration of measured I(t) and divided by the unit of charge (1.602×10^{19} As). N_{ph} is calculated as the ratio of laser pulse energy and the energy of the photon ($h\lambda/c$), where λ is wavelength, h Planck constant and c is light velocity. Laser pulse

energy is measured simultaneously with I(t) using a Si detector (Thorlabs DET10A/M), which is calibrated with a pyroelectric energy sensor (Thorlabs, ES111C). The measured pulse energy differs by a constant factor to the energy that arrives to the corannulene layer due to difference between sample dimensions and energy sensor dimensions. Therefore, the EQE is reported in arbitrary units.

References

1. Pavlica, E.; Bratina, G., Time-of-flight mobility of charge carriers in position-dependent electric field between coplanar electrodes. *Appl. Phys. Lett.* **2012,** *101* (9), 093304-5.

2. Pathipati, S. R.; Pavlica, E.; Treossi, E.; Rizzoli, R.; Veronese, G. P.; Palermo, V.; Chen, L.; Beljonne, D.; Cai, J. M.; Fasel, R.; Ruffieux, P.; Bratina, G., Modulation of charge transport properties of reduced graphene oxide by submonolayer physisorption of an organic dye. *Org. Electron.* **2013,** *14* (7), 1787-1792.

3. Pathipati, S. R.; Pavlica, E.; Schlierf, A.; El Gemayel, M.; Samorì, P.; Palermo, V.; Bratina, G., Graphene-Induced Enhancement of n-Type Mobility in Perylenediimide Thin Films. *The Journal of Physical Chemistry C* **2014,** *118* (43), 24819-24826.

4. Nawrocki, R. A.; Pavlica, E.; Ćelić, N.; Orlov, D.; Valant, M.; Mihailović, D.; Bratina, G., Fabrication of poly(3-hexylthiophene) nanowires for high-mobility transistors. *Org. Electron.* **2016,** *30*, 92-98.

5. Zhang, L.; Zhong, X.; Pavlica, E.; Li, S.; Klekachev, A.; Bratina, G.; Ebbesen, T. W.; Orgiu, E.; Samorì, P., A nanomesh scaffold for supramolecular nanowire optoelectronic devices. *Nat Nano* **2016,** *11*, 900-906.

6. Pavlica, E.; Bratina, G., Displacement current in bottom-contact organic thin-film transistor. *J. Phys. D: Appl. Phys.* **2008,** *41* (13), 135109.

7. Shockley, W., Currents to Conductors Induced by a Moving Point Charge. *J. Appl. Phys.* **1938,** *9* (10), 635-636.

8. He, Z., Review of the Shockley–Ramo theorem and its application in semiconductor gamma-ray detectors. *Nuclear Instruments and Methods in Physics Research Section A: Accelerators, Spectrometers, Detectors and Associated Equipment* **2001,** *463* (1–2), 250-267.

9. KOTOV, I., Currents induced by charges moving in semiconductor☆. *Nuclear Instruments and Methods in Physics Research Section A: Accelerators, Spectrometers, Detectors and Associated Equipment* **2005,** *539* (1-2), 267-268.